

**A multi sensor study of conditions leading to the formation of a
cyclone over Arabian Sea during 5 - 9 May, 2004**

by

M.R.RAMESH KUMAR* and P BYJU,

Physical Oceanography Division

National Institute of Oceanography

Dona Paula, Goa-403004

December 2009

Corresponding Author Address:

Dr.M.R.Ramesh Kumar,

Scientist, P.O.D, N.I.O,

Dona Paula, Goa, India – 403004.

Email:kramesh@nio.org, rameshkumar.mr@gmail.com

Tel: [91-832-2450304](tel:91-832-2450304)

Fax: [91-832-2450602](tel:91-832-2450602)

Various Abbreviations used in present study

AT	Air Temperature ($^{\circ}\text{C}$)
CS	Cyclonic Storm
CTD	Conductivity, Temperature and Depth
D	Depression
DD	Deep Depression
ECMWF	European Centre for Medium Range Weather Forecasting
IDWR	Indian Daily Weather Report
IMD	India Meteorological Department
INSAT	Indian National Satellite
MRF	Medium Range Forecast
MTRH	Mid Tropospheric Relative Humidity (%)
NCEP/NCAR	National Centre for Environmental Prediction/ National Centre for Atmospheric Research
NWP	Numerical Weather Prediction
OLR	Outgoing Longwave Radiation (Wm^{-2})
OAFlux	Objectively Analysed Air Sea Fluxes
PW	Precipitable Water (mm)
RV	Relative Vorticity (s^{-1})
SCS	Severe Cyclonic Storm
SMSWS	Sustained Maximum Surface Wind Speed (knots)
SST	Sea Surface Temperature ($^{\circ}\text{C}$)
SLP	Sea Level Pressure (hPa)
TOGA/COARE	Tropical Ocean Global Atmosphere / Coupled Ocean Atmosphere Response Experiment
TRMM	Tropical Rainfall Measuring Mission
TMI	TRMM Microwave Imager
VWS	Vertical Wind Shear (ms^{-1})
WS	Wind Speed (ms^{-1})

Abstract

The present study investigates the conditions leading to the formation of a cyclone over the Arabian Sea using in-situ, buoy, Argo floats, island, satellite, reanalysis, and blended datasets. Cyclogenesis parameters such as the Sea Surface Temperature (SST), the Mid Tropospheric Relative Humidity (MTRH), the Relative Vorticity (RV) and the Vertical Wind Shear (VWS) were examined. Further, the variability of different parameters from satellite data, such as the SST, the Outgoing Longwave Radiation (OLR), the Precipitable Water (PW), the rainfall rate, Wind Speed (WS), were also investigated from the pre-disturbance to the cyclonic stage. An analysis of the dynamic and thermodynamic cyclogenesis parameters from the reanalysis data showed that the MTRH, the RV and the PW increased dramatically from the pre disturbance stage to the depression stage by 150%, 530%, and 32% respectively. It is envisaged that better spatial and temporal satellite estimates of the OLR, the SST and the PW, blended Objectively Analysed Air Sea Flux (OAFlux), European Centre for Medium Range Weather Forecast (ECMWF) data products, and new tools, such as moored buoys and Argo floats would be useful for the study of cyclones over the Arabian Sea.

1. Introduction

Tropical cyclones are among the most destructive natural disasters of the world. About 7% of the global tropical cyclones form in the north Indian Ocean (**Gray, 1985**). Further, more number of cyclones form in the Bay of Bengal (about four times higher, **Dube et al., 1997**) than in the Arabian Sea. In the north Indian Ocean, there are two important seasons for cyclone formation, namely: a) Pre monsoon (March- May) and b) Post monsoon (October-December).

The advent of remote sensing satellites have had a major impact on our knowledge of the tropical cyclones that form over the global oceans. The location and the tracks of the systems over vast expanses of the Ocean were quite unreliable prior to the satellite era. With advances in satellite technology, more information about convective systems, their track and intensification came into light, especially over data sparse regions such as the Indian Ocean.

The present study focuses on the role of various air-sea interaction parameters, fluxes on the formation of a convective system and its intensification into a severe cyclonic storm over the Arabian Sea from the 3rd to the 10th of May, 2004. Generally, cyclones form over the south-eastern or central part of the Arabian Sea. Figure 1 depicts the track of the convective system over the Arabian Sea from the 5th to the 10th of May, 2004. (DD- Deep Depression, CS- Cyclonic Storm, SCS- Severe Cyclonic Storm) along with the position of the island station (Amini, represented by a star), moored buoy (DS 02, represented by a solid black square), and also the location of the Argo floats for the study period (represented by triangles).

The India Meteorological Department (2003) classifies the convective systems over the north Indian Ocean as: a) a low pressure system (with sustained maximum surface wind speed (SMSWS) less than 17 knots) b) Depression (SMSWS between 17-27 knots) c) Deep Depression (SMSWS between 28-33 knots) d) Cyclonic Storm (SMSWS between 34-47 knots) e) Severe Cyclonic Storms (SMSWS between 48-63 knots) f) Very Severe Cyclonic Storms (SMSWS between 64-119 knots) and g) Super Cyclonic Storm (SMSWS greater than or equal to 120 knots).

The low pressure system formed over the northern part of Sri Lanka and Tamilnadu on the 2nd and the 3rd of May lay over Kerala and its neighbouring area on the 4th of May. It moved westward, emerged into the Arabian Sea and intensified into a depression (D) at 08:30 hours Indian Standard Time (IST) over Lakshadweep (11.5°N, 73.5°S) on the 5th of May, intensified into a deep depression (DD) at 14:30 IST, and intensified into a cyclonic storm (CS) on the evening of the 5th of May at 17:30 IST within half degree latitude. The CS moved westward on the 6th of May. After that, the system moved in a northwesterly direction and intensified into a Severe Cyclonic Storm (SCS) on the 7th of May, 2004. The lowest surface pressure of the system of 984 hPa was observed on the 7th of May, 2004 at 17:30 IST and the maximum wind speed recorded was 39 ms⁻¹. The system again moved in the northwesterly direction on 8th and 9th of May and then dissipated off Sourashtra into a low pressure system. The weakening over the oceanic area could be attributed to the cold waters present over the northeastern Arabian Sea and possible dry air incursion from the northwest (Jayanthi et al, 2005).

Please place figure 1 here.

The objective of the present study is to look into the role of various ocean atmosphere parameters - prior to, during and after the cyclone transit - and its spatial distribution. The study also tries to understand, quantitatively, the drastic change of thermodynamic and dynamic genesis parameters from the pre disturbance stage to the D, the DD and the CS. Conditions during the 3rd and the 4th of May were considered as the pre disturbance phase (prior to the cyclone formation), the 5th to the 7th of May as the disturbance phase (cyclonic conditions), and the 8th and the 9th of May as the post disturbance phase (after the cyclone). In the present study, we examine two thermodynamic genesis parameters – the SST, the MTRH - and two dynamic genesis parameters – the low level RV and the VWS between the lower (850 hPa) and upper troposphere (200 hPa). In addition, we also look into the depth of the 26 °C isotherm (D26) and the cyclonic heat potential (CHP) prior to, during and after the disturbance phase of the cyclone with the available Argo floats near the cyclonic track (figure 1).

2. Data and Methodology

Various data sets used in the present study of ocean-atmosphere interactions during the cyclone on the 3rd to the 9th of May, 2004 over the eastern Arabian Sea, are given below:

2.1 NCEP/NCAR Reanalysis

The NCEP/NCAR reanalysis uses the medium range forecast (MRF) T62 model and the in-situ observations to make fine estimates of various atmospheric parameters (Kalnay et al., 1996). The reanalysis includes grid point (and spherical harmonics) values and temporal as well as spatial averages for the prescribed areas. A new method, known as optimal averaging (Gandin, 1993), has been used for the reanalysis. This method ensures minimum root mean square averaging errors, particularly important for reanalysis purposes.

The NCEP reanalysis data used in this study consists of six hourly and daily fields of various variables for the study period (from the 3rd to the 10th of May, 2004). All the fields have been interpolated to a uniform grid (2.5⁰ x 2.5⁰) amounting to 144 x 73 grid points. **The reanalysis gridded fields have been classified into four classes (A, B, C and D) depending upon the relative influence of the observational data and the model on the gridded variables. The u and v components of the wind belong to class A, indicating that this variable is strongly influence by the observed data and hence is in the most reliable class. The PW (water vapour content), on the other hand, belongs to class B, which means that although there are observational data that directly affect the value of the variable, the model also has a very strong influence on the analysis value (More details of reliability of different variables can be had from Kalnay et.al, 1996).**

2.2 Tropical Rainfall Measuring Mission/ Microwave Imager (TMI)

The various air-sea interaction parameters needed for the present study – the SST, the WS, the PW, and the rainfall - have been taken from the TRMM Microwave Imager (TMI) sensor onboard the Tropical Rainfall Measuring Mission (TRMM) satellite launched in 1997. These data sets, with a resolution of 0.25° X 0.25°, have been available since 1998. The TMI sensor

is capable of measuring the SST even in the presence of clouds. We have examined the spatial pattern of the SST, the PW and the WS before, during and after the cyclone transit from the 3rd to the 10th of May 2004 (More details of the TMI data can be had from Wentz et al., 2000).

2.3 Indian Daily Weather Report (IDWR) and DS02

The atmospheric data for the Amini Divi island station were extracted from the IDWR from the 1st to the 15th of May 2004. Various parameters, such as the SLP, the WS, the rainfall rate, and the AT from the Amini Divi island weather station, which is about 100 km south-west of the cyclogenesis area, are also used in the present study. Also, the SST, the AT, the SLP and the WS data are extracted from a moored buoy (DS02) at 10.64°N and 72.52°E, to examine the air-sea interaction processes during the cyclone period.

2.4 OA Flux

The products of the Objectively Analysed Air-Sea Fluxes (OAFlux) are constructed from different sources by an optimal blending of satellite retrievals and three atmospheric reanalyses. The OAFlux project thus improves the estimates of latent and sensible heat fluxes by using the best available surface meteorological variables and bulk algorithm (Yu, Jin and Weller et al., 2008). At present, the bulk algorithm 3.0 (Fairall et al, 2003) developed from the field experiments of the Tropical Ocean Global Atmosphere Coupled Ocean-Atmosphere Response Experiment (TOGA COARE) is used. The best possible estimates for those surface meteorological variables are obtained by applying a variational approach that seeks optimal synthesis of satellite and NWP data sources.

2.5 Blended ECMWF surface wind data

The spatial and temporal resolution of remotely sensed surface wind are blended to the operational ECMWF wind analyses over the global ocean. The method thus aims at providing 6-hourly gridded zonal and meridional wind speed and stresses on global scale. The spatial and temporal resolutions of the resulting wind fields are $0.25^{\circ} \times 0.25^{\circ}$ (in longitude and latitude) and 6 hours. They are estimated from near-real-time satellite observations (QuikScat scatterometer and SSM/I radiometers) and ECMWF operational wind analysis. The blended

products are available at synoptic time 00h:00; 06h:00; 12h:00; 18h:00 with a short delay from the real time (24 hours in a nominal mode) (More details of the data can be had from Bentamy et al., (2009)).

2.6 Outgoing longwave radiation

The outgoing longwave radiation (OLR) has been used as a proxy for convection in several studies. In the present study, we have used the interpolated OLR data provided by the NCAR/NOAA Climate Diagnostics Centre, Boulder, Colorado from their website <http://www.cdc.noaa.gov> (Liebmann and Smith, 1996). We have used the daily and the long term daily mean data to compute the OLR anomalies for the study period.

2.7 Computation of Vertical Wind Shear and Relative Vorticity

The parameter vertical wind shear is calculated as the difference in the zonal component of the wind between the pressure levels of 850 hPa (lower troposphere) and 200 hPa (upper troposphere).

$$\text{VWS} = U_{850} - U_{200} \text{ ms}^{-1}$$

And the RV is calculated using the dynamical equation

$$\text{RV} = (dV/dx) - (dU/dy) \text{ S}^{-1}$$

The zonal and the meridional components of the wind at two levels - 850 and 200 hPa - is used in the above equation for computing the RV at each level; the difference between these two levels is used in present study.

2.8 Argo Floats

Argo floats are autonomous profiling floats that are equipped with conductivity, temperature and depth (CTD) sensors that measure temperature and salinity in the ocean as a function of

the depth. We have used data from 6 Argo floats in the southeastern Arabian Sea (Figure 1) that have been profiling near the cyclone track as well as within the study period (from the 2nd to the 9th of May, 2004). Floats measuring quite close to the cyclone track were however not available during the cyclogenesis or during the rapid intensification of the system to look into the role of the CHP on the cyclogenesis (More details of the Argo floats can be had from the Argo Information centre (<http://wo.jcommops.org/cgi-bin/Webobjects/Argo>)).

3. RESULTS AND DISCUSSION

3.1 *Sea surface temperature (SST) and cooling*

In the present study, the daily TMI (Tropical Rainfall Measuring Mission (TRMM) Microwave Imager) SST data from the 3rd to the 9th of May, 2004, have been examined to see the impact of the cyclone on the SST field, since the oceanic response on the cyclones is very important in the formation and maintenance of the system. Figure 2 represents composite spatial distribution of the sea surface temperature before, during, and after the cyclone transit.

The SST was more than 30.5°C before the cyclone formation, i.e., during the 3rd and the 4th of May, 2004, over the central and eastern Arabian Sea as shown in fig.2(a). A maximum SST of 32°C was observed near the genesis area (73.5°E, 11.5°N). A moored buoy (DS02) at 10.63°N, 72.52°E, situated at about 100km southwest of the genesis area, recorded an SST maximum of 31.7°C during this period. These values are quite high as compared to the climatological mean SST of 30°C (Hastenrath and Greischar, 1989) for the month of May in the study area. The SST data from the Argo floats A2 and B3 (refer figure 1 for the location of the floats) also confirmed the presence of high SST's in excess of 30°C before the cyclogenesis. Seetaramayya and Master (1984) also observed similar high SST's (> 30°C) prior to the genesis of a monsoon depression over the east-central Arabian Sea.

During the cyclone, cells of the low SST could be seen at 13.8°N, 71.5°E to the right of the cyclone track. This is in agreement with Sadhuram (2004), who states that the rightward bias of decrease in the SST should occur due to the transit of the cyclone. According to earlier studies, the SST usually decreases to the right of the cyclone track after the transit of the cyclone. Figure 2(c) shows the TMI SST data after the cyclone transit, i.e. from the 8th to the

9th of May 2004, which shows a cooling effect in the ocean surface temperature to the left of the cyclone track. And as a whole, cooling is seen to the left of the cyclone track after the cyclone transit. A decrease in the SST by -4°C occurs during this period. The moored buoy recorded a minimum temperature of 28.5°C and a decrease of 3.2°C . The cooling tendency towards the left of the cyclone track could be attributed to the strong winds occurring to the left of the storm.

Please place figure 2 here

The wind is equatorward and parallel to the coast during this period. Wind stress may be more on the left side of the track. This may cause the oceanic surface water to drift towards the right of the wind direction, which would result in the sub-surface cold water upwelling and hence causing decrease in the SST. At the island station, Amini (10.3°N , 72.7°E) about 50km away to the southwest, recorded a wind speed of 39m/s, which agreed with the assumption that the wind was stronger to the left of the cyclone center. The strong wind on the left in the anticlockwise direction caused the ocean surface water to mix well and drift to the right of the wind direction.

In order to investigate the impact of the curl of the wind stress on the SST, we looked at the blended product of the surface wind with the ECMWF data (Bentamy et al., 2009). Figure 3 depicts the wind speed and the curl of the wind stress on the 5th of May, 2004 (for the standard synoptic hours, 00, 06, 12, and 18 GMT). The most interesting aspect is that the blended ECMWF wind product is able to depict the intensification of the convective system from the depression to the cyclonic stage quite well.

Please place figure 3 here

The vertical velocity in the Ekman layer is proportional to the curl of the wind stress. In the northern hemisphere, the positive (negative) curl will correspond to, the negative (positive) vertical velocities, or the downwelling (upwelling) of the warmer (cooler) SSTs. From figure 3, it can be seen that large positive values of the wind stress curl, indicating the

upwelling of waters over the study region. Thus we feel that the cooling of the SST over this region could be due to the combined effect of the upwelling over this region because of the very large positive wind stress curl values and increased latent and sensible heat transfer.

A convective system, such as the DD, the CS or the SCS can thus affect the thermal structure of the ocean waters in its path by cooling the surface layer of the Ocean in the wake of such a system. The surface cooling is caused primarily by wind-induced upwelling of cooler water (see figure 3) from below the surface layer. Heat loss (in the form of latent and sensible heat fluxes) across the air-sea interface and the wind-induced mixing of the surface water with those of the cooler subsurface layers also make a significant (though smaller) contribution to surface cooling.

3.2 Air-sea interaction processes during Depression

In the Arabian Sea, most of the storms are generated to the east of 67°E, between 11° to 20°N, and generally move in northerly or north-northwesterly direction and usually turn westwards, though a few recurve into the northeast. In the present study, in the cyclone formed over Arabian Sea from the 5th to the 9th of May, 2004, the D, the DD and the CS all formed on the same day (the 5th of May, 2004, see figure 1 for more details) within the half degree area of 11.5°N and 73.5°E. The depression was formed at 0830 IST, the DD at 1430 IST, and then intensified into the CS at 1730 IST.

Please place figure 4 here.

Rao et al., (1989) suggested that regions of persistent low values of OLR much below their seasonal value could be a precursor for cyclogenesis. The OLR anomaly map for the study period from the 3rd to the 8th of May, 2004 (figure 4), showed significant deepening and spreading of the OLR anomaly (convective activity) over the study area. The OLR anomaly is obtained by subtracting the long term daily mean OLR (climatological daily mean OLR) from the OLR value for each day of the study period. In this study, we have observed that the OLR anomaly values are lower than -100 Wm^{-2} (from 3rd May, 2004), which is a precursor for potential development for a convective system. The region with an OLR anomaly less than -

200 Wm^{-2} increases in size and reaches a maximum during the 6th May, 2004. A careful study of the contour map of the OLR anomaly reveals that the isopleths become steeper and closed with the intensification of the system (as can be seen for the 5th, the 6th and the 7th of May) as compared to the initial stage and post disturbance stages (i.e. the 3rd of May and the 8th of May respectively).

The OLR anomaly minima, thus corresponds to the region of maximum convection. Thus, monitoring the centre of maximum convection (OLR anomaly minima) can help us in predicting the intensification and the movement of the cyclone. However, in order to be used as a predictor for the intensification and the movement of the convective system, the OLR data that have a much better spatial and temporal resolution (e.g. Indian National Satellite (INSAT) data, which has a spatial resolution of $1^{\circ} \times 1^{\circ}$ and temporal resolution of 3 hours) than the present one ($2.5^{\circ} \times 2.5^{\circ}$; daily) should be used.

Please place Figure 5. here

The depression was observed to be formed over fairly well-mixed warm surface water ($\sim 29.5^{\circ}\text{C}$), where most of the turbulent convective processes are expected to take place. A gradual decrease in the SST (-4°C) was observed as the cyclone moved with time. Earlier studies of Price (1981) and Sadhuram (2004) noticed the rightward bias of the SST decrease. But in the present study, the decrease in the SST is seen mostly to the left of the cyclone track after the cyclone transit. By analyzing the winds, we saw that the magnitude of the air flow was higher on the left of the cyclone track and was mostly towards the south or southeast direction. This would cause an Ekman drift in the ocean and would enhance upwelling as the wind speed increases, causing the decrease in the SST. Analysis of the moored buoy data (DS02) also confirmed the decrease in the SST (figure 5). The OAF flux SST also showed a similar decrease for the study period and agreed reasonably well with the interim ECMWF data. The curve shows a gradual decrease in the SST during the period of the cyclone formation.

According to the SLP data obtained from the Amini Divi station and the nearby moored buoy (DS02), the pressure seems to be almost 1005 hPa prior to the formation of a depression, i.e. upto the 4th of May. During the conversion of depression to deep depression

and then into cyclonic storm, the pressure decreases gradually. A depression was formed with the pressure of ~ 997 hPa, and pressure further decreases during the deep depression and the cyclonic storm stages. The SLP from the ECMWF interim data also matches reasonably well with the island station and moored buoy data as can be seen from figure 5. The AT also decreased substantially during the formation of the DD and the CS. The air temperature was greater than 30°C , 1200 IST on the 3rd of May. After that, it showed, a gradual decrease; both the station and buoy recorded a minimum temperature of 23.6°C , and a decrease of $\sim 7^{\circ}\text{C}$. This indicates that cold air always advects towards the cyclogenesis area. The atmosphere gains more heat from the sea in the form of sensible heat flux; this heats the air in contact with the sea surface and produces buoyancy at the surface. The depression is formed a day after this change where the temperature is $\sim 25^{\circ}\text{C}$. During the change of depression to deep depression and then into cyclonic storm, the air temperature remains almost constant.

Seetaramayya and Master (1984), in their study, obtained a large difference between the SST and the AT to the order of 1.5°C prior to the formation of the monsoon depression, and more than 3.0°C during the system formation and thereafter. In the present study, we have also observed large differences to the order of 6.2°C prior to the formation on the 4th of May, 2004 at 0300 hours. Before the formation of the DD, this difference (between the SST and the AT) decreased to 4.2°C . It further decreased to 2.0°C with the intensification of the system, which contradicts the earlier result of Seetaramayya and Master (1984).

The wind speed showed a gradual increase during the cyclone formation. The WS was around 6 ms^{-1} before the 4th of May 0830 IST. After that, it increased drastically to a value greater than 30 ms^{-1} during depression, deep depression and cyclonic storm. The wind speed from the ECMWF data matched very well with the moored buoy data. The moored buoy recorded a much lesser magnitude in the WS than in the land station. This may be because the rough condition in the sea may have caused some sheltering affect due to huge waves.

It is observed that before the formation of the depression over the Arabian Sea, the rapid changes in the cyclogenesis parameters (Gray, 1979) occur 1 or 2 days before. The values of the MTRH, the RV, and the PW before and during the formation are given in the Table 1.

Please place Table 1. here

From the table, it can be seen that the absolute values of the MTRH, the RV and the PW show an enormous increase of 150%, 530% and 32% respectively, during the formation of the depression as compared to before. Further, the latent and the sensible heat fluxes for the study period also show significant increase in both the heat fluxes (latent and sensible) indicating its major role in the rapid intensification of the system from the DD to the CS. The distribution of these parameters is given in figure 6. Seetaramayya and Master (1986) computed the air sea fluxes in relation to the monsoon depression formed over the Arabian Sea during MONEX-79. Their study revealed that the sensible, the latent and the total heat fluxes show a substantial increase of 60, 230 and 290 $W m^{-2}$ respectively, during the formation as compared to the values obtained before the formation of the depression. Our present study does not show such a significant increase in the latent and the sensible heat flux values (table 1 and Figure 6).

Figure 6 depicts the temporal distribution of the MTRH, the RV, the PW and the heat fluxes from the 3rd to the 7th of May, 2004. The MTRH over the study area is analysed for the period before, during, and after the cyclone. We observed a marked difference between the western and eastern Arabian Sea in case of the MTRH (figure not presented). Before the tropical cyclone formation, a very dry condition existed throughout the northwestern Arabian Sea. But the southeastern part of the sea (off Kerala and Karnataka) shows an MTRH value of 70-80%, where the present cyclone was formed. It is also seen that a similar amount of mid level moisture existed in the Bay of Bengal. The higher amount of moisture over the southeastern Arabian Sea may be because of the westward flux of the moisture from the pre-existing Bay of Bengal or because there is a strong convection over the eastern Arabian Sea. In either case, an instability was created in the atmosphere which was favorable for the cyclogenesis.

During the cyclone period (figure not presented), the mid level moisture increased from 90 to 100%. On the 5th of May, about 11:30 am, the amount of mid level moisture increased from 90 to 100% over the genesis area (11.5°N, 73.5°E), which was seen to be moved towards the southwest direction as time advanced. As a whole, the highest value of

midlevel moisture was away from the center in the western and southern quadrant of the storm. A strong moisture gradient exists to the north and to the west of the cyclone. These features are expected to exert a considerable influence on the development and the movement of the tropical cyclone.

A low value of the VWS ($0-10 \text{ ms}^{-1}$) was observed before the formation of the cyclone (figure not presented). The VWS or the change of winds with height between 850 hPa and 200 hPa pressure levels, is very low. This low vertical wind shear helps the updraft of moisture and hence enhances convection. Thus low shear value traps the energy necessary for the cyclone formation without much loss to the surrounding. This would help the tropospheric warming which would increase the instability in the atmosphere to a high extent. This helps the enhancement of moist ascent from the lower layer and adds more energy to the atmosphere hence increasing the instability.

On the morning of the 5th of May, a condition favouring cyclogenesis occurred around the genesis area (11.5°N , 73.5°E), where the VWS had a value 3.5 ms^{-1} during depression. A cyclonic vortex was created under very low vertical speed shear condition. The 850 hPa westerly winds were present in a broad area to the south of this developing disturbance. These westerlies have the capability to penetrate into higher latitudes and establish environmental flow conditions conducive to disturbance intensification. That is, this flow can carry moisture from the southern part of the cyclone center, which will add more energy for the intensification. As time advances, the shear was seen to be increasing, while the depression intensified in that region. The VWS value was less than 10 ms^{-1} when the system intensified into a cyclonic storm. The cyclonic system was seen to be moving towards north, where the VWS values are low.

During the cyclone formation and intensification (figure not presented), it is clear that a high value of the RV ($9 \times 10^{-5} \text{ S}^{-1}$) is produced and that the gradient in vorticity also becomes high during the formation of the cyclone. The wind veers in the anticlockwise direction with this high value of positive RV. A higher value of RV has a greater tendency to curl, more of the air flow. The vorticity gradient is high in the northwest directions the cyclonic vortex was seen to move towards a region of higher RV gradient and the system intensified into a severe cyclonic storm. This indicates that a cyclone formation was favored in a region of high RV

and the gradient should be large. The cyclone grows as the value of the RV increases.

Please place figure 6. here

In the present study, a maximum rainfall of 116.7 cm was recorded at the land-based station, Amini, on the 6th day, which is within half degree latitude to the left of the common origin. The highest rainfall rate observed by the TMI analysis was 18 mmhr^{-1} , i.e., 43.2 cm per day. The rainfall measured by one land station is about 300% more than the satellite observation done by the TMI. The large differences between the two rainfall estimates could be due to the poor or low correlation between the TMI rainfall estimates and the island rainfall data (Ramesh Kumar et al., 2003). The study further showed that satellite estimates are not able to pick up the Intense Rainfall Events (IRE, an event when a station or a location receives more than 10 cm within a day). Further, the TMI measures the average rainfall over a region of 25 Km x 25 Km, whereas the island station data is a point observation. Rainfall is a discrete and highly variable parameter as a result of which there so much variability within the spatial resolution of the TMI rainfall data.

Argo floats provide the subsurface temperature profile and thus provide an opportunity to compute the CHP, which is one of the cyclogenesis parameter (Gray, 1979). The CHP is defined as the integrated temperature in excess of 26°C upto a depth of 26°C isotherm and computed following Sadhuram et al., (2006). The location of the various Argo floats along with the SST, depth of the 26°C (D26) isotherm and the CHP is presented in table 2. From the table, it can be clearly seen that both the D26 and the CHP increased substantially from the pre disturbance stage (the 2nd, the 3rd and the 4th of May) to the disturbance period (the 5th, the 6th, the 7th and the 8th of May), and further decreased drastically with the weakening of the system. Unfortunately, most of the Argo floats were away from the cyclone track to make any quantitative statements on the role of the CHP on the cyclogenesis.

4. Summary and conclusion

The present study investigates the conditions leading to the formation of a cyclone over the Arabian Sea using in-situ, buoy, Argo floats, island, satellite, reanalysis and blended (OAFflux, ECMWF) datasets. Cyclogenesis parameters, such as the SST, the MTRH, the RV

and the VWS were examined. Further, the variability in different parameters from satellite data such as the SST, the OLR, the PW, the rainfall rate, the WS, were also investigated from the pre disturbance to the cyclonic stage. An analysis of the dynamic and thermo dynamic cyclogenesis parameters from the reanalysis data showed that the MTRH, the RV and the PW increased dramatically from the pre disturbance stage to the depression stage by 150%, 530% and 32% respectively. It is envisaged that better spatial and temporal satellite estimates of the OLR, the SST and the PW, blended reanalysis data products (OAFflux and ECMWF), and new tools - moored buoys and Argo floats - would be useful for the study of cyclones over the Arabian Sea.

These results are preliminary in nature and we propose to use a larger dataset for a longer period (30 years) to draw conclusions for more than one cyclone. We also feel that the recently launched OCEANSAT II and the forthcoming Megha Tropiques satellite mission will provide more information.

Acknowledgements:

The freeware Ferret and the GMT were used for the analysis and preparation of the various plots. They are thankful to Dr. Gad Levy, Special Guest Editor of this issue, and to two anonymous reviewers for their useful and constructive suggestions in vastly improving an earlier version of the manuscript. They are grateful to the various agencies for providing the datasets used in the present study. This is NIO contribution number XXXX.

Figure captions.

Figure 1. Track of the cyclone from the 5th to the 10th of May 2004. (DD- deep depression, CS- cyclonic storm, SCS- severe cyclonic storm) along with the position of the island station (Amini, represented by a star), moored buoy (DS 02, represented by a solid black square) and also the location of the Argo floats for the study period (represented by triangles).

Figure.2. Maps of the TMI Sea surface temperature (a) before the cyclone (b) during cyclone and (c) after the cyclone transit. For more details read the text. The solid black line indicates the track of the cyclone.

Figure 3. Wind speed (ms^{-1}) and Wind stress curl (Nm^{-3}) over the study area for 5th May, 2004 a) 0530 hrs IST b) 1130 hrs IST c) 1730 hrs IST and d) 2400 hrs IST from blended ECMWF surface wind data.

Figure 4: The outgoing longwave radiation anomaly over the south eastern Arabian Sea for the study period from the 3rd to the 8th of May, 2004. The contour is from 80 Wm^{-2} to 220 Wm^{-2} . The contour interval is 20 Wm^{-2} . The lowest values of the OLR anomaly (OLR minima) show maximum convection.

Figure 5. The values of the sea level pressure (SLP), the air temperature (AT), the sea surface temperature (SST), the wind speed (W), the rainfall (R) collected from the land station (solid line), DS02 moored buoy (dotted line), ECMWF (solid line with triangle), OAFflux (solid line with diamond) during May, 2004. (D-depression, DD-deep depression, CS-cyclonic storm).

Figure 6. NCEP/NCAR Reanalysis data of the MTRH (%), the RV (10^{-5} S^{-1}), the PW (mm) and the latent (solid line, Wm^{-2}) and the sensible heat fluxes (dotted line, Wm^{-2}) for the study period from 3rd to the 7th of May, 2004. The values during the depression (D), the deep depression (DD) and the cyclonic storm (CS) are shown using thick arrows.

Table Legends.

Table 1. The values of the mid tropospheric relative humidity (MTRH in %) , the relative vorticity (RV in 10^{-5} S^{-1}) and the precipitable water (PW in mm) and the latent (LHF in Wm^{-2}) and the sensible heat fluxes (SHF in Wm^{-2}), 1 to 2 days before, during the depression, the deep depression and the cyclonic storm obtained from NCEP/NCAR Reanalysis and the Objectively Analysed Air Sea fluxes (OAFlux) data. (Figures written in parenthesis are the percentage increase on the values obtained before formation).

Table 2. Position of the Argo floats with date and time along with the SST ($^{\circ}\text{C}$), depth of the 26°C isotherm (D26 in m) , and the CHP, (in 10^{10} Jm^{-2}) for the period from the 2nd May to the 9th of May, 2004.

References

- BENTAMY, A., CROIZE-FILLON, D., QUEFFEULOU, P., LIU, C. and ROQUET, H., 2009, Evaluation of high –resolution surface wind products at global and regional scales. *The Journal of Operational Oceanography*, 2 (2), pp. 15-27.
- DUBE, S.K., RAO, A.D., SINHA, P.C, MURTY, T.S., and BAHULEYAN, N., 1997, Storm surge in Bay of Bengal and Arabian Sea: The problem and its prediction, *Mausam*, 48, 288-304.
- FAIRALL, C. W., BRADLEY, E.F., HARE, J.E., GRACHEV, A.A, and EDSON, J.B., 2003, Bulk parameterization on air–sea fluxes: Updates and verification for the COARE algorithm. *J. Climate.*, 16, 571–591.
- GANDIN, L. S., 1993, Optimal averaging of meteorological fields, NMC Office Note 397, 45 pp., [Available from NOAA/NCEP, 5200 Auth Rd., Washington, DC 20233].
- GRAY, W.M., 1979, Hurricanes: Their formation, structure and likely role in the tropical circulation. *Meteorology over the tropical oceans*, D. B. Shaw (Ed.), Royal Meteorological Society, James Glaisher House, Grenville Place, Bracknell, Berkshire, RG12 1BX, pp.155-218.
- GRAY, W.M., 1985, Tropical Cyclone Global Climatology, WMO Technical Document WMO/TD. No.72., Vol.1, WMO, Geneva, Switzerland, pp 3-19.
- HASTENRATH, S., and GREISCHAR, L. L., 1989, Climatic Atlas of the Indian Ocean Part III: Upper Ocean Structure, The University of Wisconsin Press, Madison, Wisconsin 53715. U.S.A. 247 charts.
- INDIA METEOROLOGICAL DEPARTMENT, 2003, Cyclone Manual, India Meteorological Department.
- JAYANTHI, N., MAZUMDAR, A.B. and SUNITHA, D.S., 2005, Cyclones and depression over north Indian Ocean during 2004. *Mousam*, 56, pp. 517-526.
- KALNAY, E., KANAMITSU, KISTLER, M.R., COLLINS, W., DEAVEN, D., GANDIN, L., IREDELL, M., SAHA, S., WHITE, G., WOLLEN, J., ZHI, Y., CHELLIAH, M, EBISUZAKI, W., HIGGINS, W. JANOWIAK, J., MO, K. C., ROPELEWSKI, C., WANG, J., LEETMAA, A., REYNOLDS, R., ROY JENNE and DENNIS JOSEPH (1996). "The NCEP/NCAR 40-Year Reanalysis Project". *Bulletin of the American Meteorological Society* 77 (3), pp. 437–471.
- LIEBMANN, B., and SMITH, C.A., 1996, Description of a complete (Interpolated) Outgoing Longwave Radiation Dataset. *Bulletin of the American Meteorological Society*, 77, pp. 1275-1277.

PRICE, J.F., 1981, Upper ocean response to hurricane. *Journal of Physical Oceanography*, **11**, pp. 153-175.

RAMESH KUMAR, M.R., SHENOI, S.S.C., and SHANKAR, D., 2003, Proceedings of the ARMEX Workshop held on 22-23 December, 2003 at NIOT, Chennai. pp 43-44.

RAO, A.V.R.K., KELKAR, R.R., and ARKIN, P.A., 1989, Estimation of precipitation and outgoing longwave radiation from INSAT 1B data, *Mausam*, 40 (2), pp. 123-130.

SADHURAM, Y., 2004, Record decrease of sea surface temperature following the passage of a super cyclone over the Bay of Bengal. *Current Science*, **86**, pp. 383-384.

SADHURAM, Y., RAMANAMURTY, T.V., and SOMAYAJULU, Y.K., 2006, Estimation of tropical cyclone heat potential in the Bay of Bengal and its role in the genesis and intensification of storms. *Indian Journal of Marine Sciences*, 35(2), pp. 132-138.

SEETARAMAYYA, P. and MASTER, A.H., 1984, Observed air sea interaction conditions and a Monsoon depression during MONEX-79. *Archives for Meteorology Geophysics and Bioclimatology Series*, **A 33**, pp. 61-67.

SEETARAMAYYA, P. and MASTER, A.H., 1986, Exchange of heat and momentum between ocean and atmosphere in relation to monsoon depression during MONEX-79. *Meteorology and Atmospheric Physics*, **35**, pp. 59-63.

YU, L., JIN, X., and WELLER, R.A 2008, Multidecade Global Flux Datasets from the Objectively Analyzed Air-sea Fluxes (OAFlux) Project: Latent and sensible heat fluxes, ocean evaporation, and related surface meteorological variables. Woods Hole Oceanographic Institution, OAFlux Project Technical Report. OA-2008-01, 64 pp. Woods Hole, Massachusetts.

WENTZ, F. J., GENTEMANN, C.L., SMITH, D.K., and CHELTON, D.B, 2000, Satellite Measurements of Sea Surface Temperature Through Clouds, *Science*, 288(5467), pp. 847-850.

Table 1. The values of the mid tropospheric relative humidity, the relative vorticity and the precipitable water 1 to 2 days before, during the depression, the deep depression and the cyclonic storm obtained from the NCEP/NCAR Reanalysis data (figures written in parenthesis are the percentage increase on the values obtained before formation).

Parameters	MTRH (%)	RV (10^{-5} S^{-1})	PW (mm)	LHF (Wm^{-2})	SHF (Wm^{-2})
1-2 day before	28.9	1.0	42.5	120.5	-3.54
depression	73 (150%)	6.4 (540%)	56.2 (32%)	123.4	-9.0
deep depression	71.3	7.30	56.30		
cyclonic storm	65.7	7.40	55.83	144.5	-19.6

Table 2. The location of the Argo floats with date and time along with the SST ($^{\circ}\text{C}$), D26 (in m), and the CHP (in 10^{10} Jm^{-2}) for the period from the 2nd May to the 9th of May, 2004.

Station No.	Latitude ($^{\circ}\text{N}$)	Longitude ($^{\circ}\text{E}$)	Date	Time	SST ($^{\circ}\text{C}$)	D26 (m)	CHP 10^{10} J m^{-2}
A2	10.504	70.398	2	17:45	30.82	85	1.037
A7	10.340	70.486	7	16:19	29.53	88	1.073
B3	11.951	68.697	3	10:03	30.10	105	1.208
B8	12.029	68.630	8	10:16	29.33	108	1.228
C5	13.979	66.997	5	13:59	29.60	60	0.713
D4	14.583	67.580	4	13:32	29.98	91	1.086
D9	14.562	67.737	9	13:52	29.30	78	0.922
E7	15.152	67.440	7	12:20	29.56	113	1.279
F3	15.961	70.885	3	10:00	29.89	68	0.740
F8	16.066	71.025	8	08:55	29.80	83	0.919

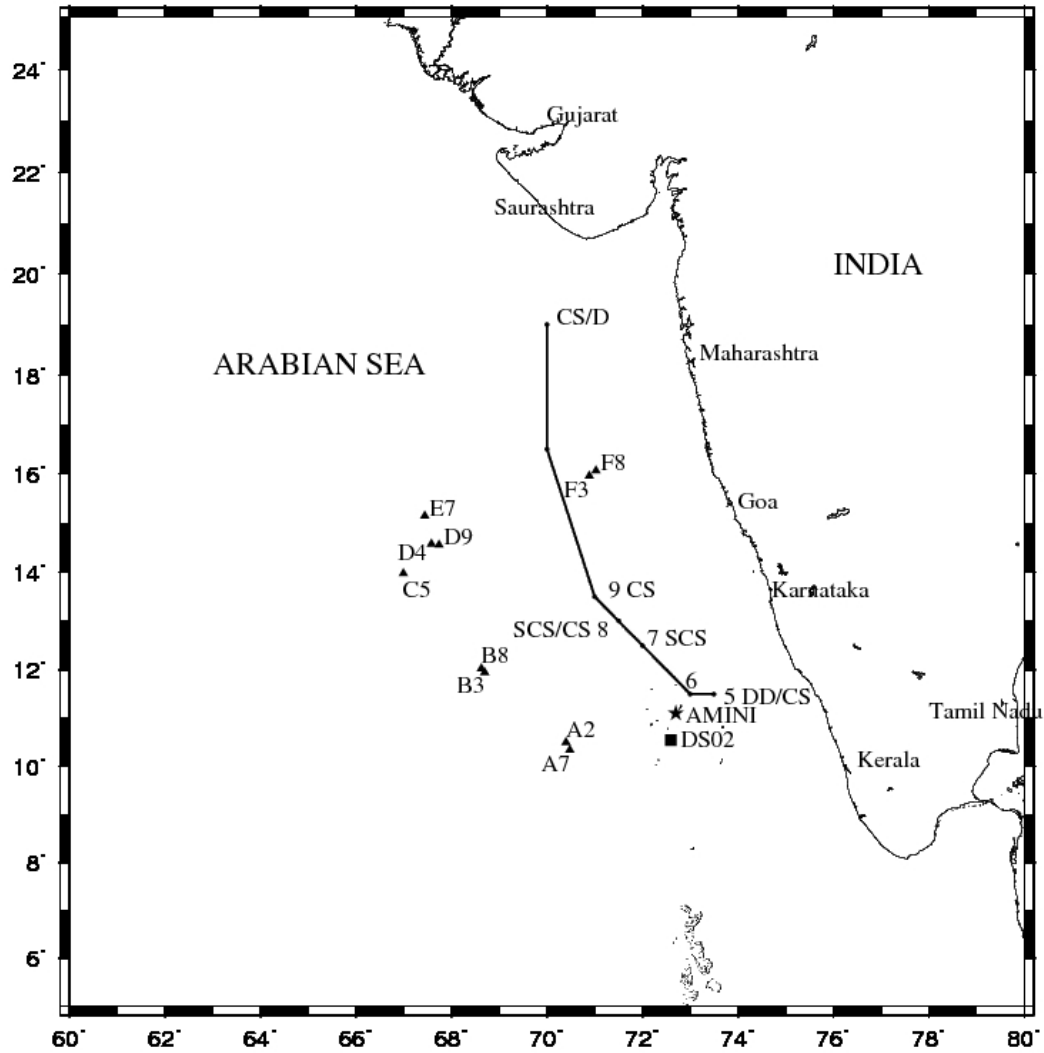


Figure 1. Track of the cyclone from the 5th to 10th of May, 2004. (DD- deep depression, CS- cyclonic storm, SCS- sever cyclonic storm) along with the position of the island station (Amini, represented by a star), moored buoy (DS 02, represented by a solid square) and also the location of the Argo floats for the study period (represented by triangles).

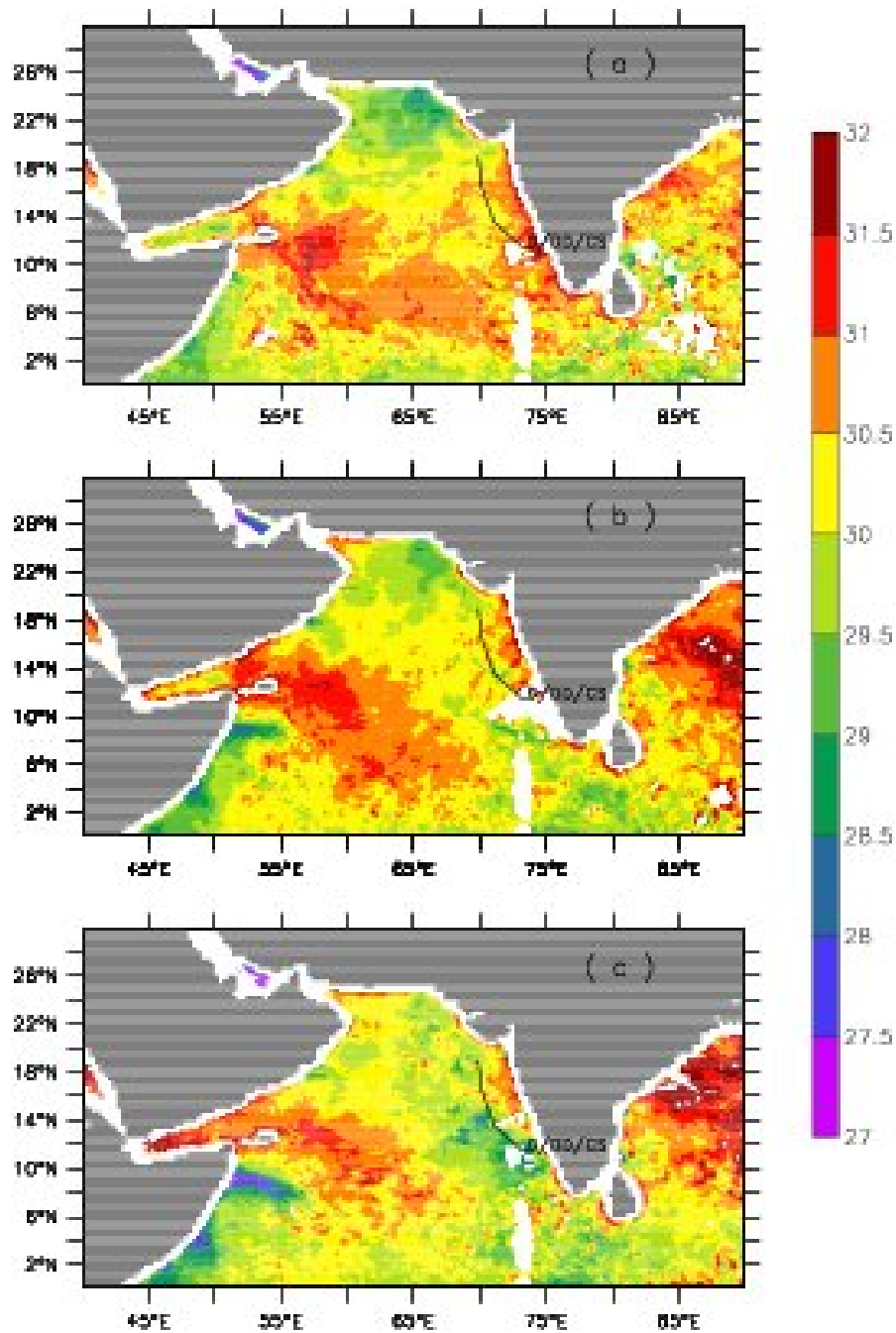


Figure.2. Maps of the TMI Sea surface temperature ($^{\circ}\text{C}$) (a) before the cyclone (b) during cyclone and (c) after the cyclone transit. The solid black line indicates the track of the cyclone.

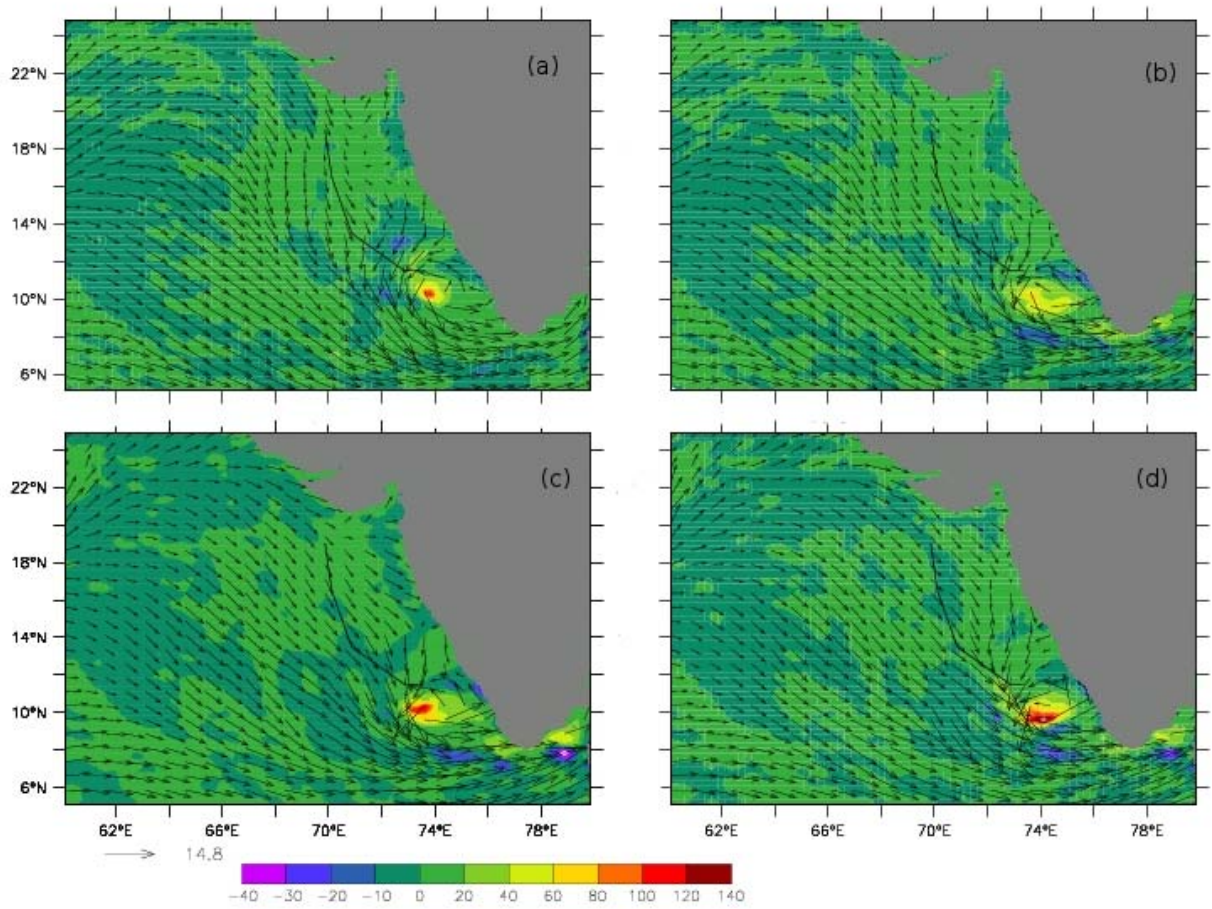


Figure 3. The wind speed (ms^{-1}) and curl of the wind stress (Nm^{-3}) over the study area for the 5th of May, 2004 a) 0530 hrs IST b) 1130 hrs IST c) 1730 hrs IST and d) 2400 hrs IST from the blended ECMWF surface wind data

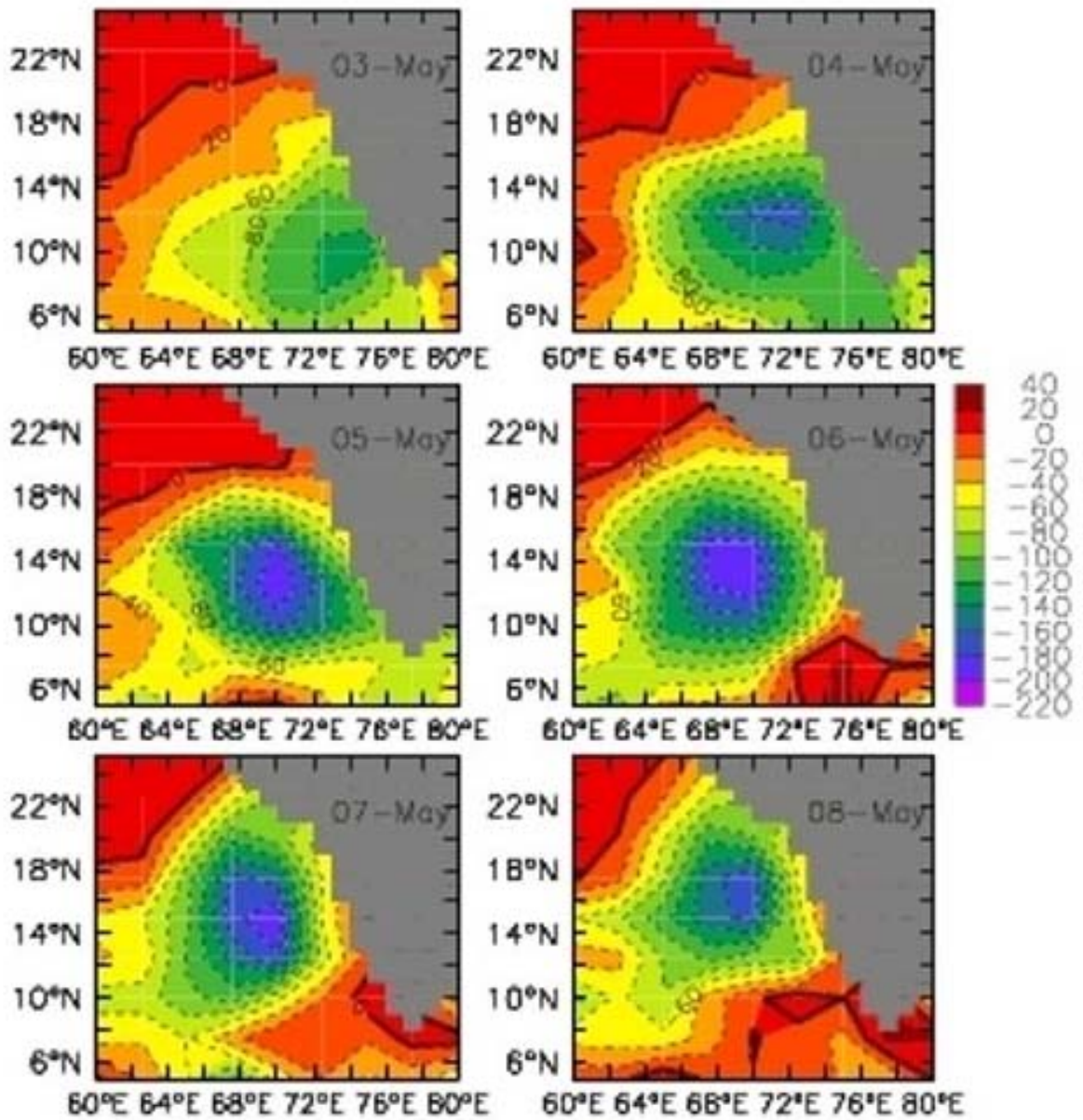


Figure 4. The outgoing longwave radiation (OLR) anomalies over the southeastern Arabian Sea for the study period from the 3rd to the 8th of May, 2004. The contour is from 40 Wm^{-2} to -220 Wm^{-2} . The contour interval is 20 Wm^{-2} .

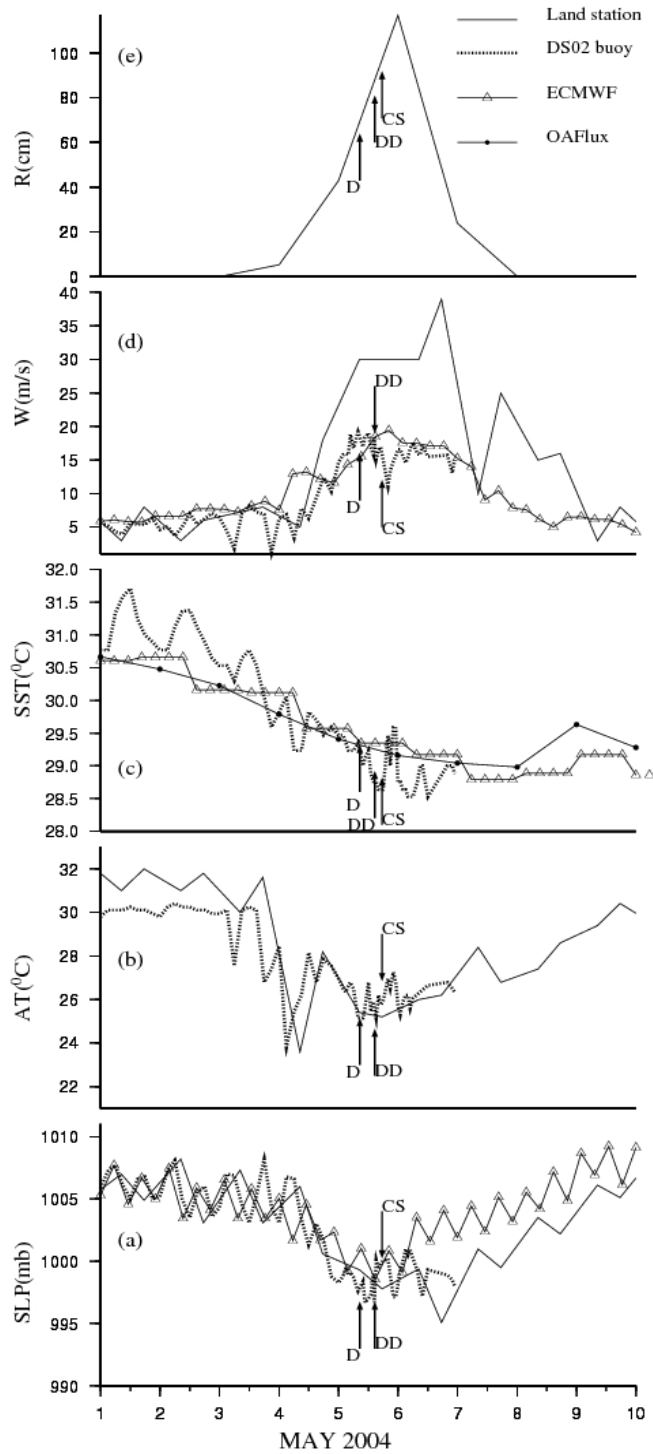


Figure 5. The values of the sea level pressure (SLP, hPa), the air temperature (AT, °C), the sea surface temperature (SST, °C), the wind speed (W , ms^{-1}), the rainfall (R , cm) collected from the land-station (solid line), DS02, the moored buoy (dotted line), the ECMWF (solid line with triangle), the OAFlux (solid line with diamond) during May, 2004.

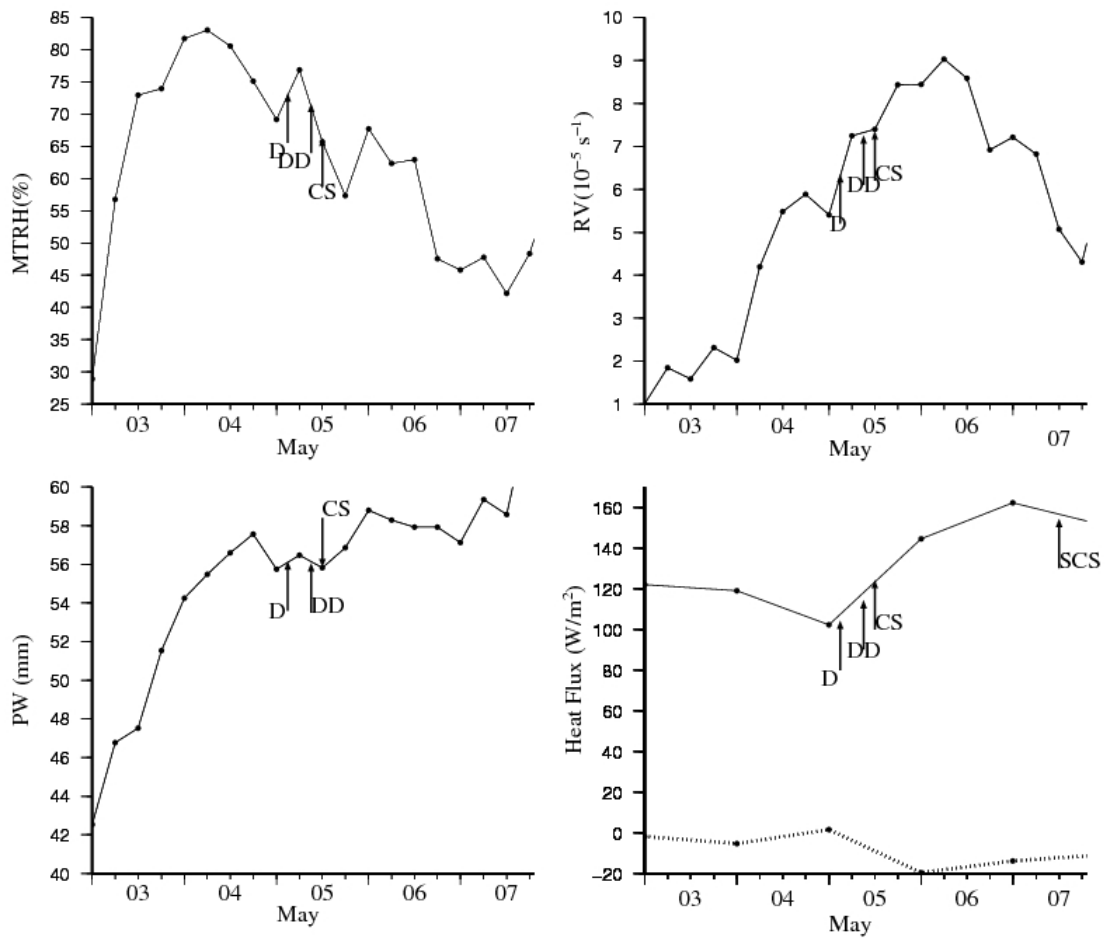


Figure 6. The NCEP/NCAR Reanalysis data of the MTRH (%), the $RV(10^{-5} \text{ S}^{-1})$, the PW (mm) and the latent (solid line, W/m^2) and the sensible heat fluxes (dotted line, W/m^2) for the study period from 3rd to the 7th of May, 2004. The values during the depression (D), the deep depression (DD) and the cyclonic storm (CS) are shown using thick arrows.